

# Spin-Torque Driven Switching Probability Density Function Asymmetry

Hui Zhao<sup>1</sup>, Yisong Zhang<sup>1</sup>, Pedram Khalili Amiri<sup>2</sup>, Jordan A. Katine<sup>3</sup>, Juergen Langer<sup>4</sup>, Hongwen Jiang<sup>5</sup>, Ilya N. Krivorotov<sup>6</sup>, Kang L. Wang<sup>2</sup>, and Jian-Ping Wang<sup>1</sup>

<sup>1</sup>Electrical and Computer Engineering, University of Minnesota, Minneapolis, MN 55455 USA

<sup>2</sup>Electrical Engineering, University of California, Los Angeles, CA 90095 USA

<sup>3</sup>Hitachi Global Storage Technologies, San Jose, CA 95135 USA

<sup>4</sup>Singulus Technologies, Kahl am Main 63796, Germany

<sup>5</sup>Physics and Astronomy, University of California, Los Angeles, CA 90095 USA

<sup>6</sup>Physics and Astronomy, University of California, Irvine, CA 92697 USA

We studied the spin transfer torque (STT) driven switching voltage distribution systematically by characterizing the switching probability density function (PDF) with large statistics ( $10^5$  trials) across a wide time scale from 5 ns to 1  $\mu$ s. The skew normal distribution function is found to be a good one to fit the measured switching PDF down to low values, which would be used as a guideline to extrapolate read disturb rate (RDR) and write error rate (WER) in STT-RAM design. Moreover, the asymmetry of switching probability density function is observed to flip when the pulse width decreases. It is related to the fluctuation mechanism transition from the thermal agitation to the initial magnetization trajectory dispersion.

**Index Terms**—Magnetic tunnel junction, spin transfer torque switching, STT-RAM.

## I. INTRODUCTION

THE spin transfer torque (STT) driven magnetization switching is the key working principle of spin transfer torque random access memory (STT-RAM) technology [1]–[5]. Early studies show that STT switching is probabilistic [6]–[8]. For functional operation, the probability that magnetization switches during the low voltage read process is referred as the read disturb rate (RDR), and the probability that the magnetization does not switch under large voltage during write process is defined as write error rate (WER) [9], [10]. Both of the two parameters are directly related to the distribution of switching voltage. Several studies have been done recently to understand the switching voltage distribution by analyzing the RDR, WER or the mean and variation of the switching voltage for STT-RAM application [11]–[18]. In this paper, we studied the switching voltage distribution more systematically by characterizing the switching probability density function (PDF) with large statistics ( $10^5$  trials) across a wide time scale from 5 ns to 1  $\mu$ s. The asymmetry of PDF was discussed.

## II. EXPERIMENT

The presented measurement results are chosen from the same in-plane MgO MTJ sample with the structure of (bottom electrode)/PtMn (15 nm)/Co<sub>70</sub>Fe<sub>30</sub> (2.5 nm)/Ru (0.85 nm)/Co<sub>40</sub>Fe<sub>40</sub>B<sub>20</sub> (2.4 nm)/MgO (0.83 nm)/Co<sub>20</sub>Fe<sub>60</sub>B<sub>20</sub> (1.8 nm)/(top electrode). The thin film stack was deposited by a Singulus TIMARIS sputtering system with 2 hours post annealing at 300°C under 1 T magnetic field. The planar shape of this particular sample is a 50 nm  $\times$  150 nm ellipse. The tunneling magnetoresistance (TMR) ratio, resistance area product (RA) and room temperature coercivity are 101%, 5.2  $\Omega \cdot \mu\text{m}^2$ , and 105 Oe respectively. The free layer shift field was canceled by

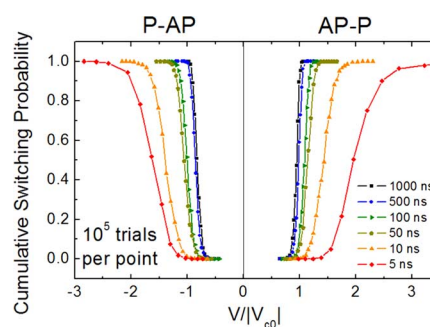


Fig. 1. Switching probability cumulative distribution function (CDF) from 5 ns to 1  $\mu$ s with  $10^5$  trials per point.

an external field during the switching probability measurement in order to center the hysteresis loop.

The switching probability measurement setup consists of two pulse generators (Picosecond 10070A, 0.1 ns–10 ns; HP 8110A, 10 ns–10 s) and a DAQ card (NI PCI-6221) synchronized to create a sequence of reset pulses, switch pulses and read pulses. The resistance was tested by the same DAQ card during the read pulse onset period through an input channel. This setup run at high testing speed up to 100 switching trials per second with relative low cost by avoiding the arbitrary wave generator (AWG) and storage oscilloscope.

## III. RESULTS AND DISCUSSION

Fig. 1 shows the measured STT switching probability cumulative distribution function (CDF) from 5 ns to 1  $\mu$ s with  $10^5$  trials per point. Both AP to P switching and P to AP switching are characterized. The switching voltage is normalized by  $V/|V_{c0}|$  in the figure, where  $V_{c0}$  is the intrinsic critical voltage fitted from the thermal activation model  $V = V_{c0}[1 - \ln(t_p/\tau_0)]/\Delta$  in the long pulse regime (1  $\mu$ s–0.1 s). In this sample,  $V_{c0,AP-P} = 0.215$  V and  $V_{c0,P-AP} = -0.273$  V.

The switching PDF, defined as the derivative of the CDF, is plotted in Fig. 2(a). As the pulse width decreases, in both AP-P and P-AP side,  $V/V_{c0}$  increases gradually from below

Manuscript received March 02, 2012; revised April 20, 2012; accepted April 27, 2012. Date of current version October 19, 2012. Corresponding author: J.-P. Wang (e-mail: jpwang@umn.edu).

Color versions of one or more of the figures in this paper are available online at <http://ieeexplore.ieee.org>.

Digital Object Identifier 10.1109/TMAG.2012.2197815

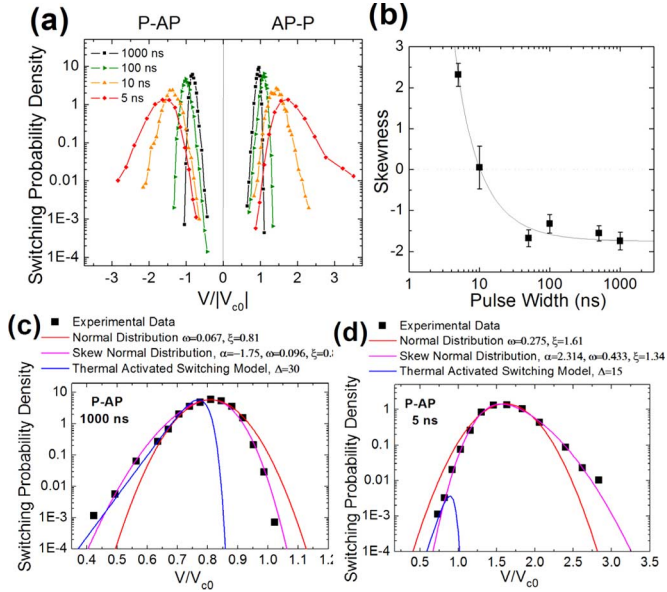


Fig. 2. (a) The switching probability density function (PDF) as the derivative of the CDF in Fig. 1; (b) Skewness value as a function of pulse width. The symbols are the experiment data fitted from the P-AP switching PDF curves and the solid curve is the guideline; (c), (d) The PDF of P-AP switching at  $1 \mu\text{s}$  and  $5 \text{ ns}$  respectively. The solid lines are the fitting of normal distribution (red), skew normal distribution (pink) and thermal activation model distribution (blue). For the thermal activation model, we used the delata value from the RDR fitting in Fig. 3(c).

1 to above 1. Meanwhile, the width of the switching PDF curve is also broadened rapidly.

The enlarged PDF curves of P-AP switching at  $1 \mu\text{s}$  and  $5 \text{ ns}$  are plotted in Fig. 2(b) and (c) respectively. Three distribution types are used to fit the experimental data. First, as expected, the classic STT switching distribution function (blue curves in Fig. 2(b) and (c)) from thermal activation model ((1) [6]–[8]) can only fit the data up to  $V/V_{c0} = 0.8$

$$p\left(\frac{V}{V_{c0}}\right) = \Delta \frac{t_p}{\tau_0 \exp(\Delta(1 - V/V_{c0}))} \cdot \exp\left(\frac{-t_p}{\tau_0 \exp(\Delta(1 - V/V_{c0}))}\right) \quad (1)$$

$$\Delta = \frac{K_U V}{k_B T}$$

Second, by comparing to the Gaussian function (red curves in Fig. 2(b) and (c)), we can see that the measured PDF curves are not symmetric. Instead, the skew normal distribution ((2)) fits the experimental data quite well down to  $10^{-3}$  in both tails (pink curves in Fig. 2(b) and (c)), and the fitted  $\alpha$  value represents the skewness of PDF asymmetry

$$f(x) = \frac{2}{\omega} \phi\left(\frac{x - \xi}{\omega}\right) \Phi\left(\alpha \left(\frac{x - \xi}{\omega}\right)\right) \quad (2)$$

where

$$\phi(x) = \frac{1}{\sqrt{2\pi}} e^{-\frac{x^2}{2}}, \Phi(x) = \int_{-\infty}^x \phi(x) dt = \frac{1}{2} \left[ 1 + \operatorname{erf}\left(\frac{x}{\sqrt{2}}\right) \right]$$

One interesting point is that the asymmetry of PDF curves switches from left skew to right skew for  $1 \mu\text{s}$  and  $5 \text{ ns}$  pulses. The same trend was observed both in AP-P and P-AP sides.

We've excluded the Ohmic heating effect in our result since no obvious temperature rising ( $> 3^\circ\text{C}$ ) was found in the pulsed switching probability measurement. The perpendicular spin torque term may have some effect on the switching probability distribution, but it cannot explain the asymmetric flip unless its magnitude oscillates with the bias voltage in both the two voltage directions. No such experimental result has been reported yet.

Therefore, the asymmetry flip is understood as a sign of the fluctuation mechanism transition from the thermal agitation to the initial magnetization trajectory dispersion. In the thermal activation mode, the switching distribution is mainly determined by the thermal agitation during the switching process. The switching CDF follows the modified Néel-Brown relaxation theory  $P = 1 - \exp(-t_p/t)$ , where  $t = \tau_0 \exp[E_0(1 - V/V_0)]$ . Mathematically, the modified Néel-Brown relaxation formula has a shape that the cumulative probability  $P$  converges to 1 much faster in the high voltage end than it converges to 0 in the low voltage end. Therefore, the PDF is always left skewed (the blue curve in Fig. 2(c)) as determined by (1).

In the precessional switching mode, the switching voltage variation is mainly dependent on the magnetization dispersion at the initial state. The smaller the switching voltage, the more precessional circles the switching trajectory will go through, and the more initial trajectory dispersion will be averaged out. As a result, there is less uncertainties in the low voltage end, leading to a steeper left tail in the plotted PDF figure. In other words, the PDF is right skewed. Therefore, we conclude that the switching voltage distribution comes from two fluctuation mechanisms: the thermal agitation during the switching process and the initial magnetization trajectory dispersion. Since the two fluctuation mechanisms have the opposite asymmetry in the switching PDF figure, we propose to use the fitted skewness value to estimate the contribution from the two fluctuation mechanisms at certain pulse width. It is particularly useful for the dynamic reversal regime, where the STT switching depends both on the thermal agitation and the initial magnetization dispersion. According to Diao *et al.*, the boundary between the dynamic reversal regime and the thermal activation regime is around  $30 \text{ ns}$  [10]. We can see that in Fig. 2(b), as the pulse width increases, the skewness has a sharp drop at first, and then reaches a relative flat stage from  $t > 50 \text{ ns}$ . This transition point is very close to the proposed boundary. Furthermore, the PDF is symmetric ( $\alpha = 0$ ) around  $10 \text{ ns}$ , corresponding to the equal contribution from the two fluctuation mechanisms.

The left tail and right tail of PDF also correspond to two crucial parameters of STT-RAM product: the RDR and the WER respectively. Fig. 3(a) and (c) show the measured RDR and WER, based on Fig. 1. In both the two figures, the RDR and WER tails become much shallower as  $V/V_{c0}$  increases to be larger than 1. It's against the fast read and write operation in ns regime for STT-RAM device as pointed out by R. Heindl *et al.* [12]. Meanwhile, we noticed a weak “low probability bifurcated branch” in the WER curve of AP-P  $5 \text{ ns}$  in Fig. 3(b) (red curve on right), similar to the case reported by Min *et al.* [13]. The bifurcated branch was found in 3 of 5 measured identical samples when  $V/V_{c0} > 2$ .

With the RDR tail down to  $10^{-5}$ , we can also fit the thermal stability factor ( $\Delta$ ) from the RDR slope as proposed by Heindl *et al.* [11]. The fitting of  $10 \text{ ns}$ ,  $100 \text{ ns}$  and  $1000 \text{ ns}$  curves are

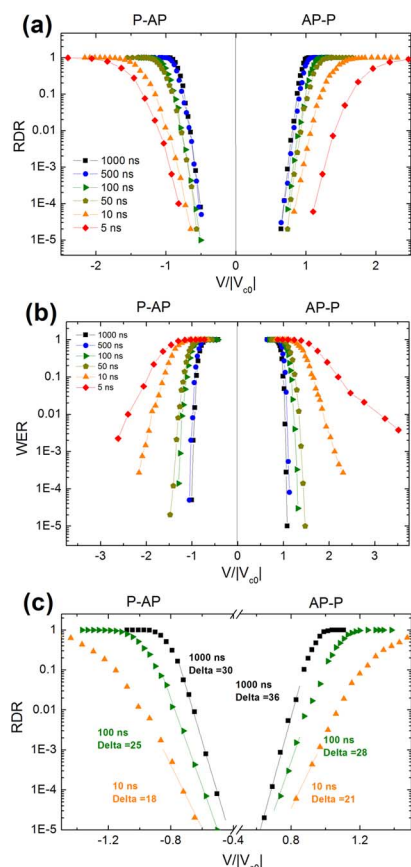


Fig. 3. (a) The Read Disturb Rate (RDR) as a function of  $V/|V_{c0}|$ ; (b) Write Error Rate (WER) as a function of  $V/|V_{c0}|$ ; (c) Evaluation of thermal stability factor from the RDR slope.

shown in Fig. 3(c). To check the fitting validation, we need to verify the premise  $t_p/t \ll 1$ , where  $t_p$  is the applied pulse width and  $t = \tau_0 \exp(\Delta(1 - V/V_{c0}))$ ,  $\tau_0 = 1$  ns [11]. Taking the P-AP side for example, when  $t_p = 1000$  ns,  $\Delta = 30$ ,  $V/V_{c0} = 0.70$ ,  $t_p/t = 0.1234$ , when  $t_p = 100$  ns,  $\Delta = 25$ ,  $V/V_{c0} = 0.75$ ,  $t_p/t = 0.1930$ , and when  $t_p = 10$  ns,  $\Delta = 18$ ,  $V/V_{c0} = 0.80$ ,  $t_p/t = 0.2732$ . All the three cases do not meet the criteria  $t_p/t \ll 1$ . Therefore, the smaller the  $t_p/t$  value, the more close the fitted thermal stability factor is compared to the statistic thermal stability factor value. It is important to do a careful check of fitting premise in order to get reasonable thermal stability factor by this method.

#### IV. CONCLUSION

The STT switching voltage distribution in MgO MTJ is studied in this paper by characterizing the switching PDF systematically with large statistics ( $10^5$  trials) in a broad time range from 5 ns to 1  $\mu$ s. It is found that the measured switching PDF can be fitted well by the skew normal distribution function down to  $10^{-3}$ , so we can use this as a guideline to extrapolate the RDR and WER in STT-RAM design. Furthermore, the measured results also show that the switching PDF curve changes from right skew to left skew as the pulse width decreases.

We propose that this phenomenon is due to the fluctuation mechanism transition from the thermal agitation to the initial magnetization trajectory dispersion. The fitted skewness value from the switching PDF is related with the contribution from the two fluctuation mechanisms. In the end, the RDR and WER tails under various pulse widths were also plotted and discussed.

#### ACKNOWLEDGMENT

This work was supported in part by the DARPA STT-RAM program (Grant No. HR0011-09-C-0114) and NSF MRSEC Program at University of Minnesota (Grants No. DMR-0819885). The work of J.-P. Wang, H. Zhao, and Y. Zhang was supported in part by an Intel University Research Grant.

#### REFERENCES

- [1] L. Berger, "Emission of spin waves by a magnetic multilayer traversed by a current," *Phys. Rev. B*, vol. 54, pp. 9353–9358, 1996.
- [2] J. C. Slonczewski, "Current-driven excitation of magnetic multilayers," *J. Magn. Mater.*, vol. 159, pp. L1–L7, 1996.
- [3] M. Tsoi *et al.*, "Excitation of a magnetic multilayer by an electric current," *Phys. Rev. Lett.*, vol. 80, pp. 4281–4284, 1998.
- [4] E. B. Myers, D. C. Ralph, J. A. Katine, R. N. Louie, and R. A. Buhrman, "Current-induced switching of domains in magnetic multilayer devices," *Science*, vol. 285, pp. 867–870, Aug. 6, 1999, 1999.
- [5] J. Z. Sun, "Current-driven magnetic switching in manganite trilayer junctions," *J. Magn. Mater.*, vol. 202, pp. 157–162, 1999.
- [6] E. B. Myers, F. J. Albert, J. C. Sankey, E. Bonet, R. A. Buhrman, and D. C. Ralph, "Thermally activated magnetic reversal induced by a spin-polarized current," *Phys. Rev. Lett.*, vol. 89, p. 196801, 2002.
- [7] Z. Li and S. Zhang, "Thermally assisted magnetization reversal in the presence of a spin-transfer torque," *Phys. Rev. B*, vol. 69, p. 134416, 2004.
- [8] R. H. Koch, J. A. Katine, and J. Z. Sun, "Time-resolved reversal of spin-transfer switching in a nanomagnet," *Phys. Rev. Lett.*, vol. 92, p. 088302, 2004.
- [9] E. Chen *et al.*, "Advances and future prospects of spin-transfer torque random access memory," *IEEE Trans. Magn.*, vol. 46, pp. 1873–1878, 2010.
- [10] Z. Diao *et al.*, "Spin-transfer torque switching in magnetic tunnel junctions and spin-transfer torque random access memory," *J. Phys.: Condens. Matter.*, vol. 19, p. 165209, 2007.
- [11] R. Heindl, W. H. Rippard, S. E. Russek, M. R. Pufall, and A. B. Kos, "Validity of the thermal activation model for spin-transfer torque switching in magnetic tunnel junctions," *J. Appl. Phys.*, vol. 109, p. 073910-5, 2011.
- [12] R. Heindl, W. H. Rippard, S. E. Russek, and A. B. Kos, "Physical limitations to efficient high-speed spin-torque switching in magnetic tunnel junctions," *Phys. Rev. B*, vol. 83, p. 054430, 2011.
- [13] T. Min *et al.*, "A study of write margin of spin torque transfer magnetic random access memory technology," *IEEE Trans. Magn.*, vol. 46, pp. 2322–2327, 2010.
- [14] X. Wang, Y. Zheng, H. Xi, and D. Dimitrov, "Thermal fluctuation effects on spin torque induced switching: Mean and variations," *J. Appl. Phys.*, vol. 103, p. 034507-4, 2008.
- [15] T. Seki, "Switching-probability distribution of spin-torque switching in MgO-based magnetic tunnel junctions," *Appl. Phys. Lett.*, vol. 99, p. 112504, 2011.
- [16] X. Wang, W. Zhu, M. Siegert, and D. Dimitrov, "Spin torque induced magnetization switching variations," *IEEE Trans. Magn.*, vol. 45, pp. 2038–2041, 2009.
- [17] M. Pakala, Y. Huai, T. Valet, Y. Ding, and Z. Diao, "Critical current distribution in spin-transfer-switched magnetic tunnel junctions," *J. Appl. Phys.*, vol. 98, p. 056107, 2005.
- [18] Y. Higo, "Thermal activation effect on spin transfer switching in magnetic tunnel junctions," *Appl. Phys. Lett.*, vol. 87, p. 082502, 2005.